

THE GIANT FLARE FROM SGR 1806–20 AND ITS RADIO AFTERGLOW

G. B. TAYLOR

*Department of Physics and Astronomy, University of New Mexico,
 Albuquerque, NM 87131, USA*

and

*National Radio Astronomy Observatory, Socorro, NM 87801, USA
 gbtaylor@unm.edu*

J. GRANOT

*Kavli Institute for Particle Astrophysics and Cosmology, Stanford University,
 P. O. Box 20450, MS 29, Stanford, CA 94309, USA*

Received 4 September 2006

The multi-wavelength observations of the 2004 December 27 Giant Flare (GF) from SGR 1806–20 and its long-lived radio afterglow are briefly reviewed. The GF appears to have been produced by a dramatic reconfiguration of the magnetic field near the surface of the neutron star, possibly accompanied by fractures in the crust. The explosive release of over 10^{46} erg (isotropic equivalent) powered a one-sided mildly relativistic outflow. The outflow produced a new expanding radio nebula that is still visible over a year after the GF. Also considered are the constraints on the total energy in the GF, the energy and mass in the outflow, and on the external density, as well as possible implications for short γ -ray bursts and potential signatures in high energy neutrinos, photons, or cosmic rays. Some possible future observations of this and other GFs are briefly discussed.

Keywords: Pulsars: individual (SGR 1806–20); stars: neutron, flare, winds; outflows; radio continuum: general.

1. Introduction

Magnetars are a small class of young, isolated, neutron stars with extremely large magnetic fields of up to $\sim 10^{15}$ G at the surface.^{11,30,41} These objects give rise to occasional bursts peaking in the hard X-ray to soft γ -ray range, thus manifesting themselves as Soft Gamma-ray Repeaters (SGRs) and Anomalous X-ray Pulsars (AXPs) (for a review see Ref. 61). They have quiescent X-ray luminosities of $\sim 10^{34}$ – 10^{35} erg s⁻¹, and are seen to pulse in the X-rays with periods of $P \sim 5$ –12 s (the pulsed fraction of the flux is ~ 5 –11% for SGRs and 4–60% for AXPs). The pulsation period is identified with the rotational period of the star. They have rapid spin-down rates, $\dot{P} \sim 10^{-11}$ – 10^{-10} s s⁻¹, leading to age estimates

of $P/2\dot{P} \sim 10^3\text{--}10^4$ yr. They have no detectable quiescent radio emission. From the rapid spin-down, and lack of any signs of accretion (e.g., infrared excess, radio emission) or orbital modulation of their emission, they are thought to be isolated (and not in binary or multiple star systems). Only 13 magnetars are known,²⁵ all in our Galaxy or the Large Magellanic Cloud (LMC) satellite galaxy.

The SGRs are more boisterous compared to the AXPs, giving rise to frequent bursts (with energies of $\lesssim 10^{41}$ erg and typical durations of ~ 0.2 s), and on rare occasions, also emit giant flares. SGRs also have somewhat larger period derivatives, and shorter spin-down ages, than AXPs. SGR-like flares have been detected from a few AXPs,²⁹ supporting the notion that SGRs and AXPs can be unified within the magnetar model.

Quite rarely, about once every ~ 50 yr per source, SGRs produce a giant flare (GF). A GF consists of a very bright initial spike that peaks in soft gamma rays (a few hundred keV) and lasts for about a quarter of a second, followed by a longer and dimmer tail that peaks in the hard X-rays (~ 10 keV) and lasts for a few hundred seconds, with a strong modulation at the rotational period of the neutron star. So far only three GFs have been detected, originating from within our galaxy or the LMC. On 1979 March 5, SGR 0526–66 in the LMC produced the first GF that could be witnessed using satellites in orbit about the Earth. The peak (isotropic equivalent) luminosity from this flare was estimated at $\sim 4 \times 10^{44}$ erg s⁻¹, which exceeds the luminosity of the entire Galaxy, for the 0.2 seconds of the peak emission. A fading tail lasted 3 minutes and exhibited strong oscillations with a period of 8.1 seconds.³⁴ The total isotropic equivalent energy release was $\sim 5 \times 10^{44}$ erg. A similar GF event was detected from SGR 1900+14 on 1998 August 27, with an isotropic equivalent peak luminosity and total energy in excess of 3×10^{44} erg s⁻¹ and 10^{44} erg, respectively. Its initial spike and tail lasted for ~ 0.35 s and ~ 400 s, respectively. A faint radio afterglow was detected in the days following this GF.¹⁸ In both of these two GFs the (isotropic equivalent) energy in the initial spike was comparable to that in the tail.

There are also some intermediate events between the short, more frequent, bursts and the giant flares, in terms of their total duration and isotropic equivalent peak luminosity and energy (see Ref. 61 and references therein). They often occur following giant flares. The largest so far of these intermediate events (on 2001 April 18, from SGR 1900+14) also showed several strong flux modulations at the stellar rotational period. All this suggests that there might be a continuum of events, differing mainly in their energy release, and consequently also in their duration and peak luminosity. It might make sense to roughly divide the different types of such events according to their isotropic equivalent energy release, E_{iso} : (i) short, more frequent, bursts ($E_{\text{iso}} \lesssim 10^{41}$ erg), (ii) intermediate events (10^{41} erg $\lesssim E_{\text{iso}} \lesssim 10^{44}$ erg), and (iii) giant flares ($E_{\text{iso}} \gtrsim 10^{44}$ erg).

The last and most spectacular of the three GFs we have witnessed so far occurred on 2004 December 27 from GSR 1806–20. The GF was preceded by a gradual change in the spectral hardness, photon index, and spin-down rate that peaked

several months in advance of the GF.⁶³ The sudden energy release of more than 10^{46} erg in gamma-rays (assuming isotropic emission at a distance of 15 kpc) managed to eject a significant amount of baryons, probably accompanied by some pairs and magnetic fields, from the neutron star.^{20,22,43} As this outflow interacted with the external medium, it powered an expanding radio nebula^{3,19} at least 500 times more luminous than the only other radio afterglow detected from an SGR GF.¹⁸

We note that the energetics are reduced by a factor of 2–6 if one adopts a lower distance of 6–10 kpc found by Cameron *et al.*⁴ based on HI absorption observations. However, a more detailed analysis by McClure-Griffiths & Gaensler³⁶ suggests that the HI observations are consistent with the X-ray absorption measurements that give a distance of 14.5 ± 1.4 kpc,⁷ and with the distance of $15.1^{+1.8}_{-1.3}$ kpc of the associated stellar cluster in G10.0–0.3.⁸ For this review we adopt a distance to SGR 1806–20 of $15 d_{15}$ kpc, so that 1 mas corresponds to $15 d_{15}$ AU or $2.25 \times 10^{14} d_{15}$ cm.

In this brief review we first consider how the GF was powered along with implications for the neutron star (Secs. 2.1–2.4), for the possible connection to short gamma-ray bursts (Sec. 2.5), and for possible signatures in high energy neutrinos, photons or cosmic rays (Sec. 2.6). We go on to discuss the radio afterglow that is still being studied over a year after the GF (Sec. 3) and its implications for the properties of the outflow from the GF and its environment. We conclude with a short discussion of possible future work (Sec. 4). The primary focus is on the observations and the immediate insights gained from them. A detailed discussion of the physics of the GF is beyond the scope of this review.

2. The Giant Flare Itself

2.1. Observational highlights

The initial spike of the GF was the brightest astrophysical transient event ever recorded (see Fig. 1, where its peak saturated the instrument and is way-off the scale), surpassing even the most intense solar flares.⁵³ In particular, it was the brightest blast of γ -rays detected in the ~ 40 years that we have had detectors

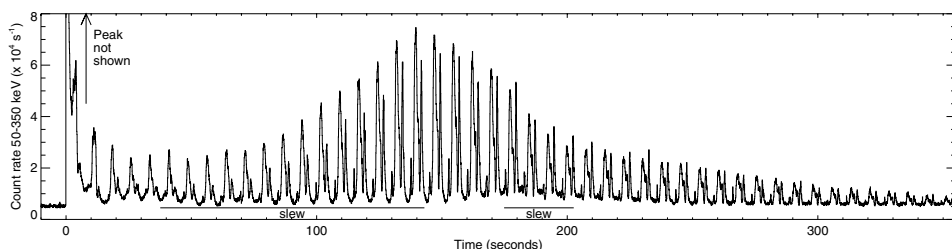


Fig. 1. Gamma-ray observations observed by SWIFT (from Ref. 43) for the first 6 minutes after the GF from SGR 1806–20. The peak of the emission is not shown, and some of the fluctuations in the count rate are due to the changing orientation of the spacecraft as it was slewing.

in orbit around the Earth. The total fluence of $\sim 1\text{--}2$ erg cm^{-2} saturated all but the least sensitive particle detectors regardless of where the γ -ray telescopes were pointed, and it created a disturbance in the Earth's ionosphere.⁵ The (isotropic equivalent) luminosity of the initial spike was $\sim (2\text{--}5) \times 10^{47} d_{15}^2$ erg s^{-1} ,^{26,43,53} or $\sim 10^3$ times that of the Galaxy, and ~ 500 times more luminous than the two previous GFs. In fact, it was so bright that even its echo off of the moon (due to Compton scattering at the moon's surface) was detected.³⁵ The isotropic equivalent energy in the initial spike was $\sim (2\text{--}5) \times 10^{46} d_{15}^2$ erg^{26,43,53} which is ~ 100 times larger than in the two previous GFs. The spectrum of the initial spike was quasi-thermal (showing an exponential cutoff at high energies and $F_\nu \propto \nu^{0.8}$ at low energies) with a temperature of $kT \approx 0.2\text{--}0.5$ MeV.^{26,43} A fading tail was detected with a strong modulation at the known rotational period of the neutron star ($P = 7.56$ s), with an isotropic equivalent energy release [$\sim (0.5\text{--}1.2) \times 10^{44} d_{15}$ erg] and duration (~ 380 s) similar to the tails of the previous two GFs.^{26,43}

A precursor to the GF was detected 142 s before the initial spike, and lasted for ~ 1 s with a flat peak.^{26,43} The initial spike was preceded by a gradual rise in the count rate which reached a moderate value (of $\sim 3 \times 10^4$ counts s^{-1} with BAT on board *Swift*) within 40 ms, at which point the main rise to the initial spike started with an exponential rise in the flux by a factor of $\sim 10^3$ within ~ 2 ms, corresponding to an e-folding time of 0.3 ms. Thus the rise time was resolved for the first time by *Swift*.⁴³ After the initial exponential rise there was at least one dip before the flux continued to rise. Later, there is evidence for two more stages of exponential flux increase with slower e-folding times of 5 ms and 70 ms.⁴⁷

2.2. *The basic current theoretical framework*

The GF is believed to have originated from a violent magnetic reconnection event in this magnetar.^{26,43,54,55} The intense internal magnetic field of $\sim 10^{16}$ G gradually unwinds and transfers helicity across the stellar surface into the magnetosphere. The stresses on the crust gradually build up until a fracture occurs, and the movement of the crust triggers a catastrophic rearrangement of the external magnetic field. The rise time and the duration of the initial spike are of the order of the Alfvén crossing time of the magnetosphere and of the star, respectively, while the duration of the tail corresponds to the cooling time of the trapped fireball.^{26,43,54,55} The intermediate ~ 5 ms time scale might be attributed to the propagation time of a ~ 5 km triggering fracture in the crust of the neutron star.⁴⁷ The observed temperature and isotropic equivalent luminosity of the initial spike suggest that the energy was released within a stellar radius or so from the surface of the neutron star.^{26,39}

The energy in the tail of the GF is believed to reflect the storage capacity of the magnetosphere, and its near constancy between the three GFs reflects the approximately similar magnetic energy between these three magnetars. This is supported by the good fit to the trapped fireball model^{54,55} of the time averaged (which takes

out the strong modulation at the rotational period of the neutron star) light curve and spectrum of the tail for the GFs from¹⁶ SGR 1900+14 and SGR 1806–20.²⁶ Any excess energy release during the initial spike, beyond the storage capacity of the magnetosphere, is channeled either into radiation (mainly soft γ -rays and hard X-rays), or into an outflow. Therefore, for very energetic events most of the energy output comes out during the initial spike, and thus the energy radiated in the initial spike can vary dramatically between different GFs (not only for different sources, as existing observations show, but also between different GFs in the same source — which cannot yet be tested observationally), reflecting the diversity in the total energy release between different events.^{26,43}

2.3. Constraints on the spin down during the giant flare

Interestingly enough, there is no change in the spin or spin-down rate associated with the GF.^{43,62,63} This is consistent with the idea that the GF is powered by a re-configuration of the magnetic field and not by tapping the rotational energy (which is insufficient anyway). Furthermore, this limits the amount of angular momentum that could have been carried away by the outflow that was launched during the GF. The extrapolation of the measurements before and after the GF to the time of the GF gives $|\Delta\nu/\nu| < 5 \times 10^{-6}$, which is significantly smaller than the spin-down of $\Delta\nu/\nu \approx -1 \times 10^{-4}$ that was measured across the 1998 August 27 GF from SGR 1900+14.⁶⁰ The spin-down during the initial spike of the 2004 December 27 GF from SGR 1806–20 might still be smaller than during its tail, despite the much larger energy in the initial spike, because the much larger luminosity in the initial spike reduces the radius out to which the outflowing material co-rotates with the star, thereby reducing its specific angular momentum.⁵⁶ Nevertheless, the strict upper limit on $|\Delta\nu/\nu|$ favors a relatively small outflowing mass, not much larger than the lower limit (of $\gtrsim 10^{24.5}$ g) that is implied by the late time radio observations.^{20,22}

2.4. QPOs in the tail and possible fracture in the crust

Quasi-periodic oscillations (QPOs) with frequencies of 18, 30.4 and 92.5 Hz have been detected in the oscillating tail of the GF²⁸ by RXTE, during part of the tail and over a certain rotational phase of the neutron star. The 92.5 Hz QPO occurred between 170 and 220 s after the initial spike, in association with a bump in the unpulsed component (corresponding to a reduction in the amplitude of the pulsations at the rotational period of the neutron star). The QPOs at 18 and 92.5 Hz have been confirmed by RHESSI⁵⁸ which also found a stronger QPO at higher energies with a frequency of 626.5 Hz that is visible at a different rotational phase. Broadly similar QPOs were also found by RXTE in the tail of the 1998 August 27 GF from SGR 1900+14.⁴⁹ Such QPOs might arise from seismic modes in the neutrons star crust that drive sheared Alfvén waves in the magnetosphere, and in particular toroidal torsional modes that might be excited by a large scale fracture

of the crust,^{21,28,45,49} which had been predicted to be excited in GFs (Ref. 10; for a different view see Ref. 32). The different rotational phase of the 626.5 Hz and 92.5 Hz QPOs might suggest an origin in different crustal fractures or magnetic reconnection events, the former associated with the main flare and the latter with the late time increase in the unpulsed emission.⁵⁸

2.5. Possible connection to short-hard gamma-ray bursts

The GF from SGR 1806–20 could have been detected by BATSE out to a distance of about 40 ± 10 Mpc.^{26,38,43} At such large extragalactic distances, only the bright initial spike would be detected, while the much dimmer pulsating tail would be below detection threshold. Given that the initial spike has a duration, variability, and energy spectrum roughly similar to gamma-ray bursts (GRBs) of the short-hard class, this raises the possibility that some fraction of the short GRBs are in fact extragalactic SGR GFs in disguise.^{26,31,38,43} There are at least three different lines of evidence which argue that the fraction f_{GF} of short-hard GRBs in the BATSE catalog that might be GFs from extragalactic SGRs is small.

First, the lack of sufficiently bright host galaxies in the error boxes of the six best localized short BATSE GRBs implies that these events are fairly distant and more energetic than GFs (with an isotropic equivalent energy release of $\gtrsim 10^{49}$ erg), and therefore $f_{\text{GF}} \lesssim 0.15$.³⁸ Second, if indeed the birth rate of magnetars follows the star formation rate (SFR; as is suggested by their relatively small inferred ages of a few thousand years) we would expect to see an excess of events from the direction of the Virgo galaxy cluster⁴³ or of nearby star forming galaxies.⁴⁶ The lack of such an excess (there is no apparent deviation from an isotropic distribution on the sky) implies $f_{\text{GF}} \lesssim 0.05$, and that either the Galactic rate of GFs as luminous as the 2004 December 27 GF from SGR 1806–20 is smaller (no more than three per millennium) than might be expected naively from the single such event that was detected so far (about three per century), or that the distance to SGR 1806–20 is ~ 6 –7 kpc instead of 15 kpc (which does not appear very likely³⁶). A third line of argument is based on the quasi-thermal spectrum of the initial spikes of GFs, which has an exponential cutoff at high energies, in contrast to the power law spectrum at high energies of almost all short-hard BATSE GRBs,³¹ which suggests $f_{\text{GF}} \lesssim 0.04$.

Interestingly enough, there is some evidence for a correlation between the directions of short-hard BATSE GRBs, and those of nearby galaxies.⁵⁰ Within 40 Mpc, this implies about $f_{\text{GF}} \approx 0.09_{-0.03}^{+0.04}$, which is marginally consistent with the upper limits mentioned above. However, there is a stronger correlation with early-type galaxies (which have a low current SFR) compared to galaxies of all types, which is strange if this correlation is indeed due to extragalactic SGR GFs. This correlation, if true, might arise more naturally in models that involve a long time delay between the star formation epoch and the onset of short GRBs, such as binary mergers, if their luminosity function is broad enough to account for the relatively low luminosities of the required nearby events.

2.6. High energy neutrinos, photons, and cosmic-rays

The huge fluence of the 2004 December 27 GF from SGR 1806–20, of $\sim 1\text{--}2 \text{ erg cm}^{-2}$, is $\sim 10^4$ times larger than that of the brightest recorded GRBs. This makes it an excellent candidate for the detection of high-energy neutrinos^{13,20,24,27} and potentially also of ultra-high energy cosmic rays² (UHECRs) or high-energy photons.¹⁴ High-energy neutrinos are expected to be produced in internal shocks within the outflow, that arise due to variations in its velocity, similar to the mechanism that had been proposed for GRBs.^{42,59} These mildly relativistic internal shocks are believed to accelerate protons to high energies, which in turn produce pions through $p\text{--}\gamma$ or $p\text{--}p$ interactions. As these pions decay they produce high-energy neutrinos and photons. Some of the shock accelerated protons may escape as UHECRs. In order for this mechanism to work efficiently in SGR GFs, the outflow must be variable and contain a significant amount of protons. Indeed, a significant amount of protons in the outflow is implied by its large mass, that is required in order to reproduce the extended coasting phase at a mildly relativistic velocity (see Sec. 3.2), while a variable outflow is suggested by the significant millisecond timescale variability seen in the initial spike of the GF from SGR 1806–20.⁴³

The expected neutrino event rates obviously depend on the model assumptions. Most works have assumed a highly relativistic outflow, while the radio observations suggest that at most $\sim 1\%$ of the total energy was in such a highly relativistic component, and most of the energy was in a mildly relativistic outflow.²² Therefore, the expected event rates may require some revisions. Recently, the IceCube collaboration has put out limits on the flux of high-energy neutrinos and photons during the GF from SGR 1806–20, using the AMANDA-II detector.¹ These limits may constrain the conditions in the outflow from the GF and call for further work. An interesting related prediction⁴⁸ is that if the internal toroidal magnetic field in newly born rapidly rotating magnetars is large enough ($\gtrsim 10^{16.5} \text{ G}$), then it would deform the star sufficiently such that its gravitational wave signal might be detected by Advanced LIGO from a magnetar as far away as the Virgo cluster. Such a high internal magnetic field, however, is more than an order of magnitude larger than that required in order to power giant flares.⁴⁰

3. The Radio Afterglow of the Giant Flare

3.1. A one-sided mildly relativistic outflow

Radio observations of SGR 1806–20 began 6.9 days after the GF, using the Very Large Array (VLA) which fortuitously was in its largest, A configuration, at the time. The high angular resolution (0.2 arcsec) afforded by the VLA in this configuration, together with its high brightness, allowed the radio afterglow to be marginally resolved by model-fitting to the visibility data. The geometric mean size measured was 57 mas, 7 days after the burst.^{4,19,52} After 30 days (the time of a rebrightening

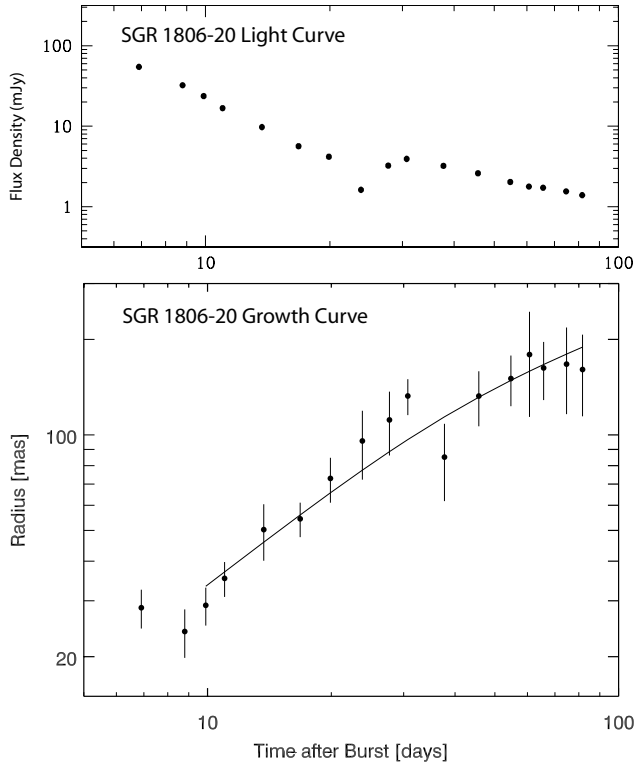


Fig. 2. Expansion of the radio afterglow from SGR 1806–20 as a function of time (adapted from Ref. 52) (bottom panel). The size shown is the geometric mean of the semi-major and semi-minor axes of the best fitting elliptical Gaussian for each observation. The solid line is a fit of a supersonically expanding shell model as described by Eq. (4) of Ref. 20. The top panel shows the 8.5 GHz light curve also from Ref. 52.

reported by Gelfand *et al.*²⁰) the radio afterglow had grown to ~ 260 mas. Between 7 and 30 days the growth of the radio nebula from 57 mas to 260 mas corresponds to an average expansion velocity of 9.0 ± 1.6 mas/day ($0.78 \pm 0.14 d_{15}c$). After this time, the growth rate appeared to slow down (see Fig. 2) so that the average expansion velocity between day 30 and day 80 is 1.0 ± 2 mas/day ($< 0.4 d_{15}c$) where the source size reached ~ 322 mas.⁵² As the radio afterglow was quite bright (170 mJy at 1.4 GHz after 7 days), it was also observed with a host of radio telescopes including MERLIN and the Very Long Baseline Array (VLBA) to provide even higher angular resolution.¹⁵ These observations revealed an elongated source with a $\sim 2 : 1$ axis ratio. The spectrum of the emission between 10 and 20 days after the GF is well fit by a single power law with slope, $\alpha = -0.75 \pm 0.02$ (where $S_\nu \propto \nu^\alpha$).¹⁹ There is some evidence for a flatter spectrum before day 10 ($\alpha = -0.62 \pm 0.02$) and a steeper spectrum after day 20 ($\alpha = -0.9 \pm 0.1$).⁴

Furthermore, the centroid of the radio afterglow from SGR 1806–20 was found to shift by ~ 200 mas over the course of the first 80 days (see Figs. 3 and 4).⁵²

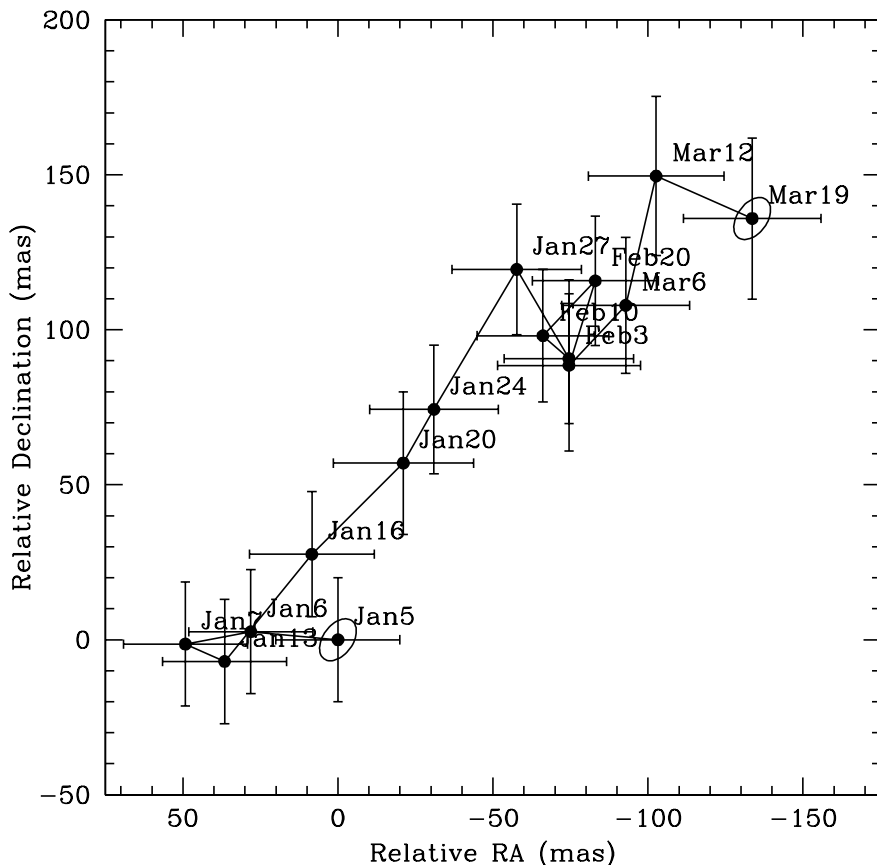


Fig. 3. The trajectory of the afterglow of SGR 1806–20 (from Ref. 52). Dates are labeled. The small ellipses denote the first and last days used.

The radial proper motion is 3.0 ± 0.34 mas/day at a position angle of $-44 \pm 6^\circ$ (measured north through east). This motion corresponds to $0.26 \pm 0.03 d_{15c}$. There is some indication that the time of fastest proper motion also corresponds to the time of fastest growth.

The motion of the radio flux centroid is along the major axis of the source and is roughly half of the growth rate. This may be naturally explained by a predominantly one-sided outflow, which produces a radio nebula extending from around the location of the magnetar out to a particular preferred direction corresponding to the direction of the ejection (Fig. 5). This suggests that either the catastrophic reconfiguration of the magnetic field which caused the GF was relatively localized, rather than a global event involving the whole magnetar (cf. Ref. 12), or that the baryonic content of the ejecta is highly asymmetric. The outflow must be intrinsically one-sided since if there was a similar “counter outflow” in the opposite direction, it should have produced significant radio emission. The collision of the observed flow

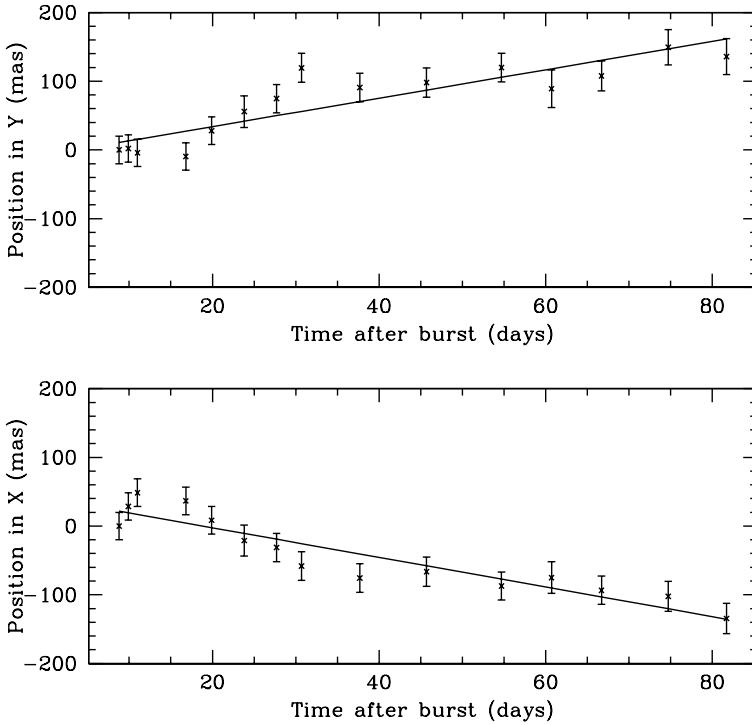


Fig. 4. Proper motion of the afterglow of SGR 1806–20. The motion has been decomposed into Right Ascension and Declination components of motion.

with the external shell occurred around $t_{\text{col}} \sim 5$ days after the GF, so in order not to detect emission from a counter outflow up to a time t after the GF, the distance of the shell (i.e. outer edge of the cavity) in the opposite direction must be at least t/t_{col} times larger. Therefore, the fact that there is no evidence for radio emission from such a counter outflow up to hundreds of days ($\sim 100t_{\text{col}}$) after the GF would require an extreme asymmetry in the external medium.

In the first 30 days, the leading edge of the one-sided expansion moves away from the magnetar position at an apparent velocity of $v_{\text{ap}} \approx 0.8 d_{15} c$.⁵² The intrinsic velocity is generally different and depends on the unknown inclination angle θ of the outflow velocity at the apparent leading edge relative to the line of sight. The minimum velocity is $v_{\text{min}} \approx 0.62c$ for an inclination angle of $\theta_{\text{min}} \approx 51^\circ$, and the true velocity is expected to be close to this value.²² Interestingly enough, this is rather similar to the escape velocity of $v_{\text{esc}} \approx 0.5c$ from a neutron star. At these mildly relativistic velocities (minimal Lorentz factor $\Gamma_{\text{min}} \approx 1.3$) there is a modest increase in the total kinetic energy for such a wide one-sided outflow compared to simple estimates based on a spherical outflow.²⁰ The total kinetic energy increases by a factor of ~ 2 –3, owing to the factor ~ 2 higher velocity at the leading edge but lower velocities elsewhere, while the isotropic equivalent kinetic energy increases by

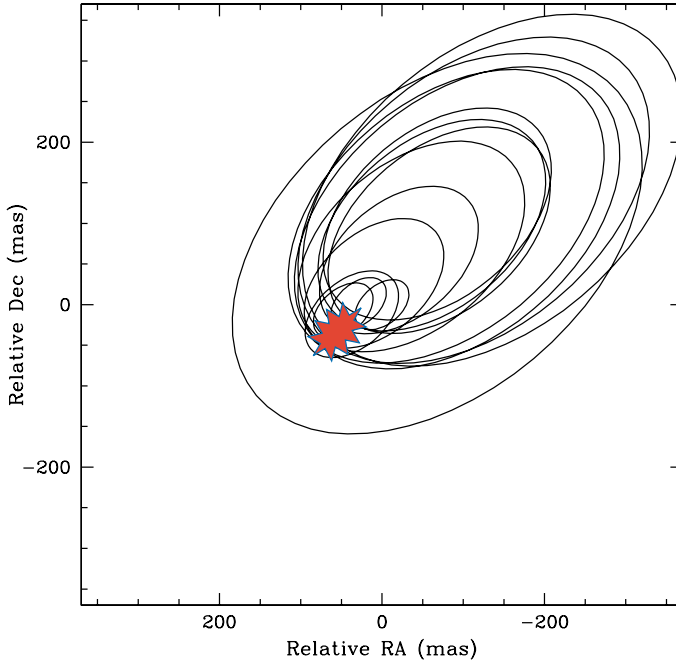


Fig. 5. A schematic of the growth and motion of the radio afterglow from SGR 1806–20 with time. The best fitting elliptical fits are drawn for each epoch, properly centered on the derived position. The position of the initial explosion is illustrated in the shaded part.

a larger factor.²² This leads to a revised estimate for the total kinetic energy in the ejecta of $\gtrsim 10^{44.5}$ ergs. By momentum conservation, a one-sided outflow of²² $10^{24.5}$ g at $0.62c$ imparts a kick to the magnetar of $21(M_*/1.4 M_\odot)^{-1}$ cm s⁻¹ where M_* is the mass of the neutron star (such a low kick velocity would be very hard to detect).

The outflow does not remain (mildly) relativistic indefinitely. Following Gelfand *et al.*²⁰ (see their Eq. (4)), the data from day 9 onwards is reasonably fit by a model featuring a supersonically expanding spherical shell that is decelerated as it sweeps up material.⁵² While the deceleration of an anisotropic outflow might be somewhat different than in the spherical case, the latter may still serve as a rough approximation. The fit (reduced χ^2 of 0.76; shown as the solid line in Fig. 2) implies a deceleration time of 40 ± 13 days after the GF, consistent with the time of the peak rebrightening at ~ 33 days (see upper panel of Fig. 2).

3.2. The underlying dynamical model

Here we present a simple dynamical model that can naturally account for the radio observations.^{19,20,22} The reader is referred to the literature for alternative views,^{9,33,57,64} which in our view are not as successful in explaining all of the radio observations.

If the electrons that emit in the radio at the time of the first observation (6.9 days), at a distance of $\sim 10^{16}$ cm from the neutron star, had been accelerated near the neutron star (whose radius is $\sim 10^6$ cm), then they would have suffered huge adiabatic losses, thus requiring an exceedingly large initial energy. In addition, in the first 2–3 days of radio observations (taken 7–9 days after the GF) the flux was still rounding off ($\sim t^{-1.5}$) before reaching the asymptotic steeper power law decay ($\sim t^{-2.7}$) that lasted until ~ 25 days. This suggests that the radio emission lit up slightly before the first observation (i.e. around ~ 5 days), as a result of a collision between the outflow that was ejected during the initial spike of the GF and an external shell. Such an external shell naturally results due to the bow shock that is formed by the quiescent relativistic pulsar-type wind of the neutron star as it moves supersonically through the ambient medium.^{19,22}

During the collision the external shell is swept up by a forward shock while the outflow is slightly decelerated by a reverse shock. After the collision the merged shell keeps propagating outwards at a constant coasting speed, and gradually sweeps up an increasing amount of external medium. Initially the emission is dominated by the electrons of the shocked shells. After the forward and reverse shocks finish crossing these shells there is no fresh supply of shock accelerated electrons and the emitting electrons cool adiabatically while the magnetic field in the shell decreases as the shell expands outwards to larger radii. This naturally accounts for the steep decay of $\sim t^{-3}$ until ~ 25 days.^{19,20,22} Figure 6 illustrates the underlying geometry in this model.

As an increasing mass of external medium is swept up, the emission from the newly shock accelerated electrons within the shocked external medium rises with time, until eventually (at around ~ 25 days) it starts to dominate over the rapidly decaying emission from the merged shocked shell. When the mass of the swept-up external medium exceeds that of the merged shell, most of the energy has been transferred to the shocked external medium and the flow starts to significantly decelerate, naturally producing a peak in the radio light curve (at ~ 33 days), followed by a more moderate flux decay.^{20,22} The fact that the deceleration in the apparent expansion speed coincides with the peak of the bump in the radio light curve (see Fig. 2) nicely supports this model.

In order to reproduce the observed coasting phase at a constant mildly relativistic apparent expansion velocity over a factor of ~ 4 –5 in radius, the bulk of the original outflow (in terms of mass and energy) could not have been ultra-relativistic, and must have instead been only mildly relativistic with a velocity very close to that observed during the coasting phase, i.e. $\sim 0.7c$ at the leading edge.²² This also implies a large baryonic mass ($\gtrsim 10^{24.5}$ g) in the outflow which, if spread uniformly over the outflow, would have obscured the first ~ 30 s of the pulsating tail of the GF. The fact that such an obscuration did not occur suggests an anisotropic distribution of baryons in the outflow, where our line of sight was relatively baryon-poor (and radiation-rich, in order to see a bright initial spike).²² A similar requirement arises in order to produce the quasi-thermal initial spike.³⁹ This could be manifested, e.g., either if the baryons are concentrated in a large number of clumps or

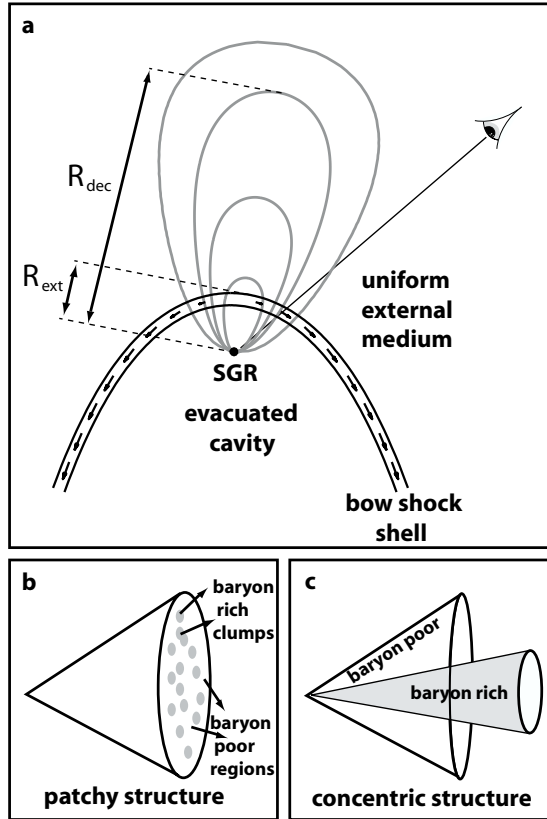


Fig. 6. Illustration of the basic underlying geometry in the dynamical model (from Ref. 22). (a) A pre-existing shell surrounding a cavity (i.e. an evacuated region) is formed due to the interaction of the SGR quiescent wind with the external medium, and the SGR’s supersonic motion relative to the external medium. The outflow from the SGR 1806–20 GF was ejected mainly in one preferred direction, probably not aligned with the head of the bow shock (which is in the direction of the SGR’s systemic motion). The ejecta collide with the external shell at a radius R_{ext} , and then the merged shell of shocked ejecta and shocked swept up external shell continues to move outward at a constant (mildly relativistic) velocity. As it coasts outward, it gradually sweeps up the external medium until at a radius $R_{\text{dec}} \sim (4\text{--}5)R_{\text{ext}}$ it has accumulated a sufficient mass to be significantly decelerated. At $R > R_{\text{dec}}$ the structure of the flow gradually approaches the spherical self-similar Sedov–Taylor solution. (b, c) Most of the mass in the outflow was in baryons that were decoupled from the radiation, and our line of sight was baryon-poor. This naturally occurs if there are separate baryon-rich (radiation-poor) and baryon-poor (radiation-rich) regions. Such regions might consist of small baryon-rich clumps surrounded by baryon-poor regions (b) or might alternatively be part of a global large-scale, possibly concentric configuration (c).

by some more ordered global configuration of the outflow (see panels b and c in Fig. 6).

3.3. Linear polarization

Linear polarization from the radio afterglow was detected during the first 20 days after the GF at 8.5 GHz.^{19,52} Thereafter only upper limits on the polarization⁵²

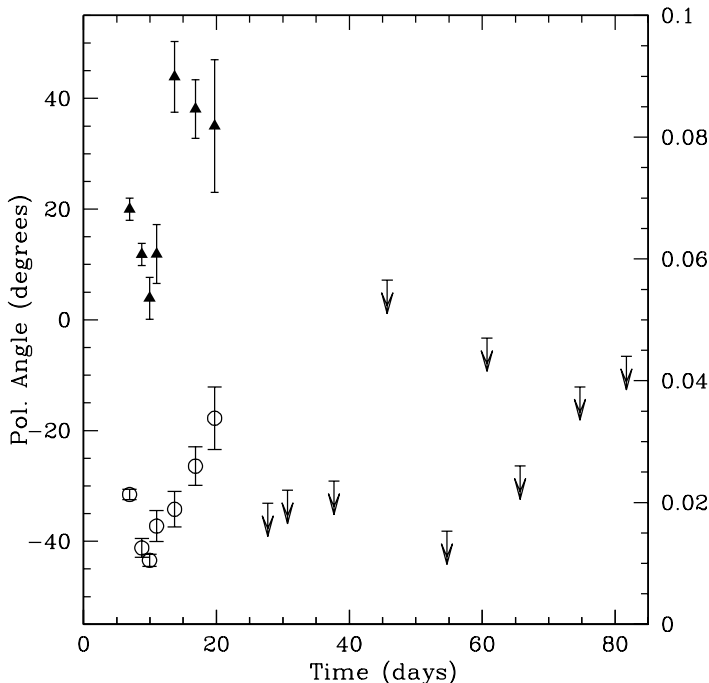


Fig. 7. Linear fractional polarization (circles; right y -axis) and polarization angles (triangles; left y -axis) for the radio afterglow of the giant flare from SGR 1806–20 as a function of time at 8.5 GHz (from Ref. 52). All polarization angles have been corrected for the observed RM of 272 ± 10 rad m^{-2} .¹⁹ Limits on fractional polarization are drawn at 3σ .

could be set (see Fig. 7). The polarization is found to be 2.1% on day 7 and it decreases to a minimum of 1.1% on day 10. At that time the linear polarization began to increase steadily up to a maximum value of 3.4% on day 20 while the polarization angle swung rapidly from 4° to 40° . The polarization falls below our detection limit of 2% around the time of the rebrightening in the light curve. Limits as late as 55 days after the GF are below 2%.⁵² The measured linear polarization and the spectral shape strongly suggest that synchrotron radiation dominates the radio emission.

During the first 20 days of high polarization, the emission is attributed to the shocked ejecta and a shocked external shell.^{19,20,22} If the emission is mostly from the shocked ejecta, then the degree of polarization of a few percent suggests that the magnetic field in the ejecta is not dominated by a magnetic field component ordered on large scales, but is instead tangled on relatively small scales. A similar conclusion is reached for GRB outflows, from “radio flare” observations.²³ Alternatively, if the emission is dominated by the shocked external shell (as suggested by the dynamics)²² then the degree of polarization of a few percent might suggest that the doubly shocked material in the external shell has a magnetic field that is not predominantly ordered on large scales.

The degree of polarization decreased around the same time when the emission started to be dominated by the shocked external medium. This suggests a lower degree of polarization in this component, and in turn that the magnetic field in the shocked external medium is less ordered than that in the shocked ejecta and/or in the shocked external shell.⁵²

The position angle of the linear polarization is roughly perpendicular to the major axis of the image and to the direction of motion of the flux centroid. Because of the elongated shape of the emitting region and due to projection effects,¹⁹ such a polarization may naturally arise for a shock-produced magnetic field. This assumes that such a magnetic field is tangled predominantly within the plane of the shock, as expected from a simple linear stability analysis,³⁷ and manages to survive in the bulk of the shocked fluid (which is not obvious). Alternatively, such a polarization might be caused by shearing motion along the sides of the one-sided outflow, which can stretch the magnetic field in the emitting region along its direction of motion.

3.4. *Beaming and energetics*

It is usually argued that, unlike GRBs, the initial γ -ray spike of GFs is not significantly beamed. The main argument for this is as follows. The strong modulation of the tail emission with the rotational period of the neutron star implies that it is emitted by material that is confined to the neutron star and co-rotates with it. This argues against strong beaming of the tail emission (although some degree of anisotropy is still required in order to produce the observed pulsations). Furthermore, the pulsating tail of the GFs from Galactic SGRs (or SGR 0526–66 in the LMC) is bright enough to be detected even without the initial spike. Nevertheless, there is no observed pulsating tail without a bright initial spike (with an isotropic equivalent energy output at least comparable to that in the tail). Such “spikeless tails” should, however, be observed if the initial spike of GFs was strongly beamed into a solid angle $\Delta\Omega < 4\pi$ and had a negligible (isotropic equivalent) luminosity outside of this solid angle, for lines of sight outside of $\Delta\Omega$ (in fact, they should even be more frequent than the observed GFs which have an initial spike, for a significant beaming where $\Delta\Omega < 2\pi$).

However, one should keep in mind that in practice such a simple picture might not be very realistic, and if the luminosity outside of $\Delta\Omega$ was smaller than inside $\Delta\Omega$ by a large but finite factor, $f_L \gg 1$, rather than being totally negligible, then this might explain the lack of “spikeless tails”, as well as the difference in the isotropic equivalent luminosity and energy in the initial spike of the GF from SGR 1806–20 compared to that of the two previous GFs. The peak isotropic equivalent luminosity of initial spike of the GF from SGR 1806–20 was several hundred times larger than that of the previous two GFs, suggesting that $f_L \sim 10^2$ – 10^3 . The current event rate statistics (one out of three giant flares observed so far from within $\Delta\Omega$ under this interpretation) suggest $4\pi/\Delta\Omega \lesssim 100$. Therefore, there is a significant uncertainty on the degree of beaming of the initial spike, which implies a similar

uncertainty on the true energy that was radiated during the GF (by a factor of up to ~ 100).

There is, however, a somewhat better handle on the kinetic energy of the outflow from the radio afterglow. The expanding radio nebula provides a more robust calorimeter for the kinetic energy output of the GF. Reproducing the observed synchrotron flux and the size of the radio nebula around the peak of the bump in the light curve at ~ 33 days provides lower limits on the energy ($E \gtrsim 10^{44.5}$ erg) and mass ($M \gtrsim 10^{24.5}$ g) of the outflow, as well as on the external density ($n \gtrsim 10^{-2.3}$ cm $^{-3}$).^{20,22} Since the source size and velocity are measured directly, only the external density n is missing in order to determine the total mass M and energy E (which both scale linearly with n). The lower limits above correspond to the minimal energy that produces the observed synchrotron flux when the fraction of internal energy in the relativistic electrons (ε_e) and in the magnetic field (ε_B) in the shocked external medium reach equipartition values. An upper limit on n , M , and E may be obtained by the requirement that the synchrotron self-absorption frequency is below ~ 240 MHz at ~ 30 days, as implied by low frequency radio observations,⁴ and that $\varepsilon_B \gtrsim 10^{-3}$ (or that $\varepsilon_e \gtrsim 0.025$): $n \lesssim 0.5(\varepsilon_B/10^{-3})^{-0.4}$ cm $^{-3}$, $M \lesssim 10^{26.5}(\varepsilon_B/10^{-3})^{-0.4}$ g, and $E \lesssim 10^{46.5}(\varepsilon_B/10^{-3})^{-0.4}$ erg (Gelfand *et al.* in prep.).

4. Future Work

Recent A-configuration observations with the VLA should provide a good image of the resolved afterglow one year after the GF. It will be interesting to look for signs of limb brightening, or circularization away from the 2:1 axis ratio seen in the early period of rapid growth. Owing to the brightness of the afterglow, its slow decay, and improvements planned for the VLA, this afterglow could potentially be studied for the next 15 years. Deep Chandra observations will also look for the presence of an X-ray nebula.

More detailed modeling of the dynamics of the interaction between the outflow and its surrounding, including a special relativistic 2D and 3D hydrodynamic calculations are already underway (Ramirez-Ruiz *et al.* in prep.), and the effects of magnetic fields are also considered. Together with better resolution of the radio image with the VLA in its A-configuration, this can provide better constraints on the properties of the outflow from the GF, and on its immediate environment.

This event provides a unique opportunity to study the evolution of a collisionless shock that is initially mildly relativistic, as it decelerates and becomes increasingly Newtonian. A detailed study of the radio light curve and spectrum, as well as the evolution of the source size and morphology, can provide valuable information on the evolution of the shock microphysical parameters in this interesting dynamical range around the transition between relativistic and Newtonian shocks (Gelfand *et al.* in prep.), bridging the gap between gamma-ray burst (GRB) afterglows and supernova remnants.

The recent limits from AMANDA-II on the flux of high-energy neutrinos and photons from the SGR 1806–20 GF¹ can be used to constrain the physical properties of the outflow. This could potentially have interesting implications for the efficiency of neutrino production and/or the acceleration of UHECRs in the internal shocks of GRBs.

Ultra-high energy cosmic rays (UHECRs) from the SGR 1806–20 GF could in principle arrive at the Earth from its direction years after the event, and might be detected by AUGER if the deflection of the UHECRs by Galactic magnetic fields is not too large.² This can be tested by AUGER in the years to come.

Acknowledgments

We thank Bryan Gaensler for helpful suggestions at the outset of this work and Ehud Nakar for useful comments on the manuscript. G.B.T. thanks Pablo Parkinson at UCSC for inviting him to give the talk at the SCIPP seminar series on which this review was initially based. This research was supported by the US Department of Energy under contract DEAC03-76SF00515 (JG).

References

1. A. Achtenberg *et al.*, astro-ph/0607233.
2. K. Asano, R. Yamazaki and N. Sugiyama, *Publ. Astron. Soc. Pac.* **58**, L7 (2006).
3. P. B. Cameron and S. R. Kulkarni, *GCN Circ.* 2928 (2005).
4. P. B. Cameron *et al.*, *Nature* **434**, 1112 (2005).
5. P. Campbell *et al.*, *GRB Coord. Network* **2932**, 1 (2005).
6. P. Chandra, *GCN Circ.* 2947 (2005).
7. S. Corbel, P. Wallyn, T. M. Dame, P. Durouchoux, W. A. Mahoney, O. Vilhu and J. E. Grindlay, *Ap. J.* **478**, 624 (1997).
8. S. Corbel and S. S. Eikenberry, *Astron. Astrophys.* **419**, 191 (2004).
9. Z. G. Dai, X. F. Wu, X. Y. Wang, Y. F. Huang and B. Zhang, *Ap. J.* **629**, L81 (2005).
10. R. C. Duncan, *Ap. J.* **498**, L45 (1998).
11. R. C. Duncan and C. Thompson, *Ap. J.* **392**, L9 (1992).
12. D. Eichler, *Mon. Not. R. Astron. Soc.* **335**, 883 (2002).
13. D. Eichler, astro-ph/0504452.
14. Y. Z. Fan, B. Zhang and D. M. Wei, *Mon. Not. R. Astron. Soc.* **361**, 965 (2005).
15. R. P. Fender *et al.*, *Mon. Not. R. Astron. Soc.* **367**, L6 (2006).
16. M. Feroci, K. Hurley, R. Duncan and C. Thompson, *Ap. J.* **549**, 1021 (2001).
17. D. A. Frail, G. Vasisht and S. R. Kulkarni, *Ap. J.* **480**, L129 (1997).
18. D. A. Frail, S. R. Kulkarni and J. S. Bloom, *Nature* **398**, 127 (1999).
19. B. M. Gaensler *et al.*, *Nature* **434**, 1108 (1999).
20. J. D. Gelfand *et al.*, *Ap. J.* **634**, 89 (2005).
21. K. Glampedakis, L. Samuelsson and N. Andersson, *Mon. Not. R. Astron. Soc. Lett.* **371**, L74 (2006).
22. J. Granot *et al.*, *Ap. J.* **638**, 391 (2006).
23. J. Granot and G. B. Taylor, *Ap. J.* **625**, 263 (2005).
24. F. Halzen, H. Landsman and T. Montaruli, astro-ph/0503348.
25. A. K. Harding, astro-ph/0510134.
26. K. Hurley *et al.*, *Nature* **434**, 1098 (2005).

27. K. Ioka, S. Razzaque, S. Kobayashi and P. Mészáros, *Ap. J.* **633**, 1013 (2005).
28. G. L. Israel *et al.*, *Ap. J.* **628**, L53 (2005).
29. V. M. Kaspi, F. P. Gavriil, P. M. Woods, J. B. Jensen, M. S. E. Roberts and D. Chakrabarty, *Ap. J.* **588**, L93 (2003).
30. C. Kouveliotou *et al.*, *Nature* **393**, 235 (1998).
31. D. Lazzati, G. Ghirlanda and G. Ghisellini, *Mon. Not. R. Astron. Soc.* **362**, L8 (2005).
32. Y. Levin, *Mon. Not. R. Astron. Soc.* **368**, L35 (2006).
33. M. Lyutikov, *Mon. Not. R. Astron. Soc.* **367**, 1594 (2006).
34. E. P. Mazets, S. V. Golenetskij and Y. A. Guryan, *Sov. Astron. Lett.* **5**, 343 (1979).
35. E. P. Mazets, T. L. Cline, R. L. Aptekar, D. D. Frederiks, S. V. Golenetskii, V. N. Il'inskii and V. D. Pal'shin, astro-ph/0502541.
36. N. M. McClure-Griffiths and B. M. Gaensler, *Ap. J.* **630**, L161 (2005).
37. M. V. Medvedev and A. Loeb, *Ap. J.* **526**, 697 (1999).
38. E. Nakar, A. Gal-Yam, T. Piran and D. B. Fox, *Ap. J.* **640**, 849 (2006).
39. E. Nakar, T. Piran and R. Sari, *Ap. J.* **635**, 516 (2005).
40. E. O. Ofek, submitted to *Ap. J.*
41. B. Paczyński, *Acta Astron.* **42**, 145 (1992).
42. B. Paczyński and G. Xu, *Ap. J.* **427**, 708 (1994).
43. D. M. Palmer *et al.*, *Nature* **434**, 1107 (2005).
44. T. J. Pearson, *ASP Conf. Ser. 180: Synthesis Imaging in Radio Astronomy II* (Astron. Soc. Pacific, 1999), p. 335.
45. A. L. Piro, *Ap. J.* **634**, L153 (2005).
46. S. B. Popov and B. E. Stern, *Mon. Not. R. Astron. Soc.* **365**, 885 (2006).
47. S. J. Schwartz *et al.*, *Ap. J.* **627**, L129 (2005).
48. L. Stella, S. Dall'Osso and G. L. Israel, *Ap. J.* **634**, L165 (2005).
49. T. E. Strohmayer and A. L. Watts, *Ap. J.* **632**, L111 (2005).
50. N. R. Tanvir, R. Chapman, A. J. Levan and R. S. Priddey, *Nature* **438**, 991 (2005).
51. G. B. Taylor, D. A. Frail, E. Berger and S. R. Kulkarni, *Ap. J.* **609**, L1 (2004).
52. G. B. Taylor *et al.*, *Ap. J.* **634**, L93 (2005).
53. T. Terasawa *et al.*, *Nature* **434**, 1110 (2005).
54. C. Thompson and R. Duncan, *Mon. Not. R. Astron. Soc.* **275**, 255 (1995).
55. C. Thompson and R. Duncan, *Ap. J.* **561**, 980 (2001).
56. C. Thompson, R. C. Duncan, P. M. Woods, C. Kouveliotou, M. H. Finger and J. van Paradijs, *Ap. J.* **543**, 340 (2000).
57. X. Y. Wang, X. F. Wu, Y. Z. Fan, Z. G. Dai and B. Zhang, *Ap. J.* **623**, L29 (2005).
58. A. L. Watts and T. E. Strohmayer, *Ap. J.* **637**, L117 (2006).
59. E. Waxman and J. N. Bahcall, *Phys. Rev. Lett.* **78**, 2292 (1997).
60. P. M. Woods *et al.*, *Ap. J.* **524**, L55 (1999).
61. P. M. Woods and C. Thompson, astro-ph/0406133.
62. P. M. Woods, C. Kouveliotou, E. Gogus, M. Finger, S. Patel, J. Swank and K. Hurley, *Astron. Tele.* **407**, 1 (2005).
63. P. M. Woods, C. Kouveliotou, M. H. Finger, E. Gogus, C. A. Wilson, S. K. Patel, K. Hurley and J. H. Swank, astro-ph/0602402, to appear in *Ap. J.*
64. R. Yamazaki, K. Ioka, F. Takahara and N. Shibazaki, *Publ. Astron. Soc. Pac.* **57**, L11 (2005).